Reduction of the tyrosyl radical and the iron center in protein R2 of ribonucleotide reductase from mouse, herpes simplex virus and *E. coli* by *p*-alkoxyphenols

Stephan Pötsch[a,b,*], Margareta Sahlin[b], Yves Langelier[e], Astrid Gräslund[d], Günter Lassmann[a,b]

[a]*Max-Delbrück-Center of Molecular Medicine, Robert-Rössle-Str. 10, D-13122 Berlin, Germany*
[b]*Max-Volmer-Institute of Biophysical and Physical Chemistry, Technical University of Berlin, D-10623 Berlin, Germany*
[c]*Department of Molecular Biology, Stockholm University, Arrhenius Laboratories, S-10691 Stockholm, Sweden*
[d]*Department of Biophysics, Stockholm University, Arrhenius Laboratories, S-10691 Stockholm, Sweden*
[e]*Institut du Cancer de Montréal, Hôpital Notre-Dame, Montréal, Québec H2L 4M1, Canada*

Received 27 July 1995; revised version received 11 September 1995

Abstract **The rate of reduction of the tyrosyl radical in the small subunit of ribonucleotide reductase (protein R2) from *E. coli*, mouse, and herpes simplex virus (HSV-2) by a series of *p*-alkoxyphenols with different alkyl chains, have been studied by stopped-flow UV-vis and stopped-flow EPR spectroscopy. The reduction and release of iron in R2 by the inhibitors was followed using bathophenanthroline as chelator of Fe^{2+}. *p*-Alkoxyphenols reduce the mouse R2 tyrosyl radical 1–2 orders of magnitude faster than the HSV-2 and *E. coli* radical. In contrast to *E. coli*, the iron center in R2 from mouse and HSV-2 is reduced by the inhibitors. For mouse R2, the rate of reduction of the tyrosyl radical increases in parallel with increasing alkyl chain length of the inhibitor, an observation which may be important for the design of new antiproliferative drugs.**

Key words: Ribonucleotide reductase; *p*-Alkoxyphenol; Kinetic

1. Introduction

The enzyme ribonucleotide reductase (RR, E.C. 1.17.4.1) is essential for DNA-synthesis, since it catalyses the reduction of ribonucleotides to their corresponding deoxyribonucleotides. The catalytically active enzyme of class I RR is a 1:1 complex of two non-identical homodimeric proteins R1 and R2. Class I RR's are found in mammals, in some DNA viruses such as herpes simplex virus (HSV), and in some bacteria, e.g. *E. coli*. Protein R1 has binding sites for substrates and allosteric regulators. The active form of protein R2 harbours one tyrosyl radical, and one μ-oxo-bridged binuclear ferric iron site per polypeptide chain. The iron/radical center can be detected by UV-vis spectroscopy showing a sharp peak around 410 nm, characteristic for the tyrosyl radical, and a band at 370 nm, arising mainly from the iron center. The tyrosyl radical exhibits a characteristic EPR doublet signal at $g = 2.0047$. The activity of RR is directly proportional to the amount of tyrosyl radical in protein R2 [1–6]. The three-dimensional crystal structure of *E. coli* R2 (2.2 Å resolution) has shown that the tyrosyl radical/iron site is deeply buried inside the protein, about 10 Å distant from the nearest protein surface, and is surrounded by several hydrophobic amino acid residues [7].

Since the activity of RR is maximal in the early S-phase of proliferating cells, this enzyme represents an important potential target for new antiproliferative drugs [8]. A recent study (EPR spectroscopic inhibition assays) has shown that derivatives of the depigmenting drug 4-hydroxyanisole, which has earlier been used for treatment of malignant melanoma [9], are highly effective for inactivating mammalian R2 (IC_{50}: 0.5–11 μM), in cell-free protein extract as well as in whole tumor cells (Ehrlich ascites). As for hydroxyurea (HU), which is a well-known inhibitor of RR, the mechanism is presumably a 1-electron reduction. The most potent agent, *p*-propoxyphenol, inactivates mammalian R2 protein 215-fold more effectively than *E. coli* R2. The inactivation of mammalian R2 increases significantly with the length of the hydrophobic alkyl side chain of the inhibitors [10]. Previous studies of protein R2 with inhibitors, e.g. HU for mouse R2 [11] and catechol for HSV-2 [12] have shown that the reduction of the tyrosyl radical is accompanied by a reduction and subsequent loss of the iron center for the mouse and the virus R2 proteins.

The aim of the present paper is to study mechanisms of inactivation of protein R2 of RR by a series of *p*-alkoxyphenols with varying alkyl chain length using kinetic techniques of EPR and UV-vis spectroscopy. The rates of reduction of the tyrosyl radical in the R2 proteins from *E. coli*, mouse, and HSV-2 are compared. The different reactivities of the iron site in the three proteins by *p*-alkoxyphenols are studied.

2. Materials and methods

Hydroxyurea, bathophenanthroline-disulfonic acid and *p*-methoxyphenol were purchased from Sigma; *p*-ethoxyphenol, *p-n*-propoxyphenol, *p-n*-butoxyphenol, and potassium nitrosodisulfonate (Fremy's salt) were purchased from Aldrich; *p-iso*-propoxyphenol, *p-iso*-butoxyphenol, and *p*-allyloxyphenol [4-(2-propenyloxy) phenol] were synthesized by Dr. W. Radeck, WITEGA-Laboratorium Berlin- Adlershof GmbH. Solutions of the inhibitors were prepared in 50 mM Tris-buffer, pH 7.6, 0.1 M KCl, or 50 mM HEPES-buffer, pH 7.7 buffer containing <1% dimethylsulfoxide. Dithiothreitol (DTT) was purchased from Serva.

Active protein R2 from *Escherichia coli* was prepared from an overproducing *E. coli* strain [13]. Recombinant mouse R2 protein was prepared as previously reported [14]. The tyrosyl radical/iron site in mouse R2 protein was regenerated anaerobically by addition of ferrous iron

*Corresponding author. Fax: (49) (30) 9494161.
E-mail: epr@orion.rz.mdc-berlin.de

Abbrevations: DNA, deoxyribonucleic acid; DTT, dithiothreitol; EPR, electron paramagnetic resonance; HSV-2, herpes simplex virus type 2; I, spin quantum number; RR, ribonucleotide reductase.

SSDI 0014-5793(95)01082-3

(Fe/R2 = 6) and oxygen to the apoprotein [15]. Both proteins were kept and studied in 50 mM Tris, pH 7.6, 0.1 M KCl. The HSV-2 ribonucleotide reductase R2 subunit was produced in a procaryotic expression system by the pET-R2 vector. The purified R2 was activated by adding ferrous iron (Fe/R2 = 6) to the protein diluted in 50 mM HEPES, pH 7.7 containing 50 mM DTT under aerobic conditions and then it was passed on a G25 column to remove unbound iron. The protein concentrations were determined with the Bradford colorimetric assay [16] or with the absorbance index, $\varepsilon_{280-310}$ = 124,000 $M^{-1} \cdot cm^{-1}$ for mouse R2, 120,000 $M^{-1} \cdot cm^{-1}$ for *E. coli* R2, and 104,000 $M^{-1} \cdot cm^{-1}$ for HSV-2 R2, respectively [14].

A DX.17MV BioSequential stopped-flow spectrofluorimeter from Applied Photophysics was used for time-resolved light absorption experiments with recombinant mouse R2 and HSV-2 R2 proteins (10–20 μM each) with the inhibitor 1 mM at 20°C. A volume of 55 μl of each reactant was needed per 1 : 1 mixing shot.

A stopped-flow EPR accessory, type SFA1, especially designed for biological applications [17], linked with an EPR spectrometer (Bruker ESP 300E) was used to follow the kinetics of the reaction of the tyrosyl 122 radical in *E. coli* R2 protein (50 μM) with the inhibitor (1 mM) at room temperature. 70 μl of each reactant was used per 1 : 1 mixing shot.

Light absorption spectra of mouse R2, HSV-2 R2, and *E. coli* R2 (10–20 μM each), respectively, with or without the inhibitor in the wavelength range 250–700 nm were recorded on a spectrophotometer (Perkin Elmer Lambda 2) using a thermostated water bath.

Anaerobic reactions were performed to study the reduction of the iron center in the protein R2. An anaerobic cuvette was filled with 500 μl of 50 mM Tris, pH 7.6, 0.1 M KCl containing the inhibitor (50–500 μM final concentration) and bathophenanthroline (500 μM). Thereafter, this solution was bubbled with argon for at least 2 h. The reaction was then started by the addition of the protein R2 to the solution in the cuvette.

3. Results

3.1. Reaction of the tyrosyl radical in protein R2 with p-alkoxyphenols

The tyrosyl radical in *E. coli* R2 exhibits a well detectable EPR doublet at room temperature (Fig. 1A inset) hence the kinetics of its destruction can be followed by EPR stopped-flow technique [17]. In mouse R2 [17] and HSV-2 R2, the tyrosyl EPR signal is visible at room temperature, but considerably broadened to a less intense singlet with line widths around 10 mT due to a stronger magnetic interaction with the iron center. Therefore, the kinetics of the loss of the tyrosyl radical in mouse and HSV-2 R2 were preferentially studied with optical stopped-flow technique monitoring the 417 nm and the 410 nm peak, respectively [11,12].

The reactivity of the tyrosyl radical in the R2 proteins towards the different *para*-substituted alkoxyphenols (methoxy-, ethoxy-, propoxy-, *iso*-propoxy-, butoxy-, *iso*-butoxy-, allyloxyphenol) at room temperature was investigated. HU was used as a reference inhibitor. Fig. 1A shows the EPR kinetics for *E. coli* R2 with *p*-propoxyphenol. The rate of quenching of the tyrosyl radical by all *p*-alkoxyphenols and HU follows pseudo-first order kinetics in excess of the inhibitors. The rate constants k_2 of quenching the tyrosyl radical in *E. coli* R2 at 20°C are summarised in Table 1. The results show that *p*-alkoxyphenols with larger unbranched alkyl groups react faster with the tyrosyl radical in *E. coli* R2 than HU (k_2 = 0.36 $M^{-1} \cdot s^{-1}$). The fastest rate with *E. coli* R2 was found for *p*-butoxyphenol (k_2 = 3.5 $M^{-1} \cdot s^{-1}$) which is 3.9 faster than for *p*-methoxyphenol. Inhibitors with a branched side-chain show a significant lower reactivity than the straight chain isomer, e.g. for *p-n-* and *p-iso*-propoxyphenol by a factor of 3 and for *p-n-* and *p-iso*-butoxyphenol by a factor of 9 (Table 1).

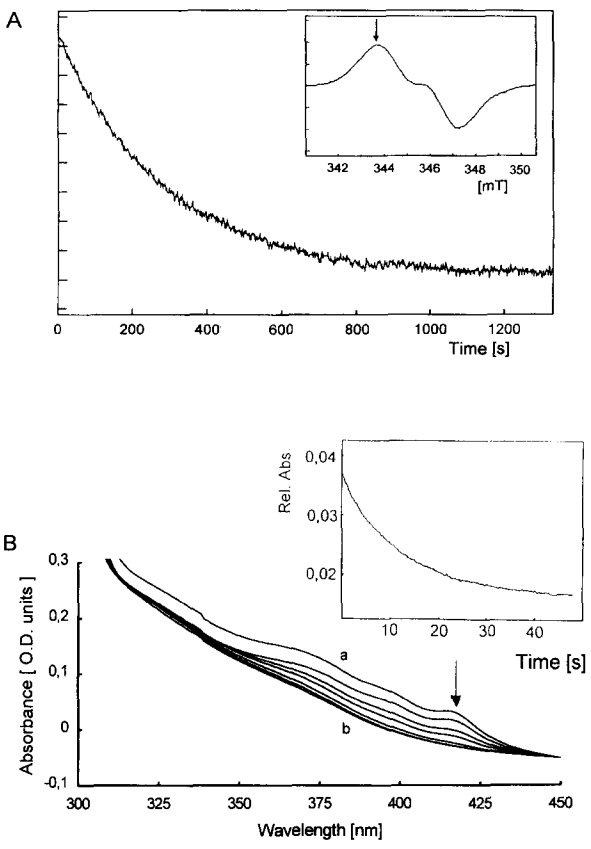

Fig. 1. (A) Kinetic of reduction of the tyrosyl radical after a 1 : 1 mixing shot of *E. coli* R2 (50 μM) with *p-n*-propoxyphenol (10 mM) measured at the top of spectrum (arrow) in the EPR stopped-flow apparatus (parameter settings: modulation amplitude = 1 mT; microwave power = 40 mW; time constant = 1.3 s). Inset: EPR spectrum of the tyrosyl radical for *E. coli* R2 (50 μM) at 20°C measured in a cylindrical stopped flow cell (parameter settings: modulation amplitude = 1 mT; micro-wave power = 40 mW; time constant = 0.3 s; sweep time = 41 s). (B) Light absorption spectra at 10°C in the range of 300–450 nm for mouse R2 (15 μM) upon the reduction by *p-n*-propoxyphenol (50 μM). Spectra were recorded after reaction times of 0 (a); 0.5; 3; 6; 9; 15; 30 and 60 min (b). Inset: Stopped-flow kinetic trace at 417 nm following the reduction of the tyrosyl radical of mouse R2 (15 μM) with *p*-propoxyphenol (1 mM) at 20°C.

Nearly the same rate constants of quenching the tyrosyl radical in *E. coli* R2 by *p-iso*-propoxyphenol and *p-iso*butoxyphenol were found when the experiments were carried out in a stopped-flow UV-vis apparatus (Table 1), showing that the reproducibility of the kinetic data are independent of the method of analysis.

Light absorption spectra of the mouse R2 protein, showing characteristic bands associated with the tyrosyl radical/iron center, were recorded after addition of *p*-alkoxyphenols with different alkyl chains. The plots recorded after different times with *p*-propoxyphenol (Fig. 1B) show a decrease of the absorption at 417 nm (tyrosyl radical) as well as at 370 nm (iron site) [11]. The kinetics of the absorbance at 417 nm was used to follow the reduction of the tyrosyl radical by *p*-alkoxyphenols.

The rate of quenching the tyrosyl radical follows pseudo-first order kinetics for all compounds (inset of Fig. 1B). Table 1 shows the rate constants of reduction of the tyrosyl radical in recombinant mouse R2 protein by *p*-alkoxyphenols and HU at

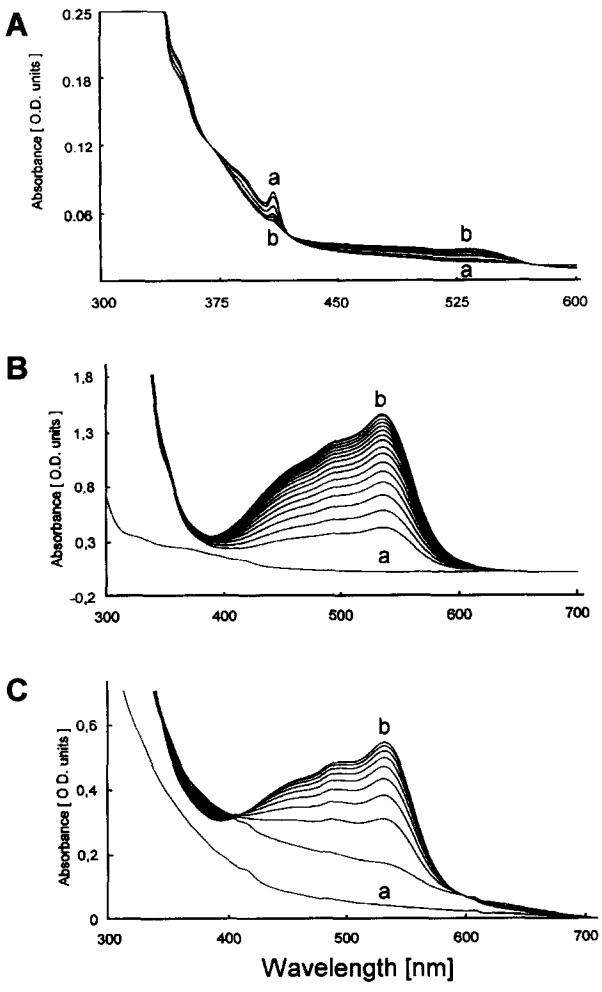

Fig. 2. Light absorption spectra in the range of 250–700 nm of different proteins R2 after the reduction by *p-n*-propoxyphenol (0.5 mM) in presence of bathophenanthroline (500 μM) under anaerobic conditions. For mouse R2 and HSV-2 R2 protein, the experiments were performed at a lower temperature to suppress the effect of spontanious loss of the tyrosyl radical. (A) *E. coli* R2 (20 μM) at 20°C; spectra were recorded after reaction times of 0.5 (a); 9; 35; 65; 85; and 120 min (b). (B) Mouse R2 (18 μM) at 10°C; spectra were recorded after reaction times of 0 (a); every 15 min up to 240 min (b). (C) HSV-2 R2 (20 μM) at 10°C; spectra were recorded after reaction times of 0 (a); 0.5; 20; and then every 20 min up to 160 min (b).
←

20°C. The rate constants increase with increasing size of the hydrophobic alkyl side group of the *p*-alkoxyphenols. The factor of increase was 9.5 from the methyl to the butyl derivative. The rate constant is also influenced by the side-chain branching showing an increase for the *iso*-propyl over *n*-propyl derivatives, but *iso*-butyl shows a slight decrease compared to the *n*-butyl derivative. The most potent inhibitor for tyrosyl radical reduction is again the *p*-butoxyphenol (k_2 = 267 $M^{-1} \cdot s^{-1}$), 243-fold more potent than HU (k_2 = 1.1 $M^{-1} \cdot s^{-1}$). Substitution in the *para*-position of the phenol ring enhances the reactivity of the inhibitor compared with substitution in the *ortho*-position, e.g. *p-iso*-propoxyphenol reduced the tyrosyl radical about 25-fold more effectively than the *ortho*-substituted compound *o-iso*-propoxyphenol (Table 1).

The temperature dependence of the second order rate constant for the reaction of *p-iso*-butoxyphenol with the mouse R2 was studied in the temperature range 15–26°C. From the slope of the Arrhenius-plot, an activation energy of 13 kJ/mol was estimated (data not shown).

The reduction of the tyrosyl radical in HSV-2 R2 by *p*-alkoxyphenols and HU was studied by stopped-flow UV-vis absorption spectroscopy at 410 nm [12]. All *p*-alkoxyphenols react faster with the HSV-2 R2 tyrosyl radical than HU. Although the most active derivatives are the *n*-ethyl- and *n*-butyl derivatives in HSV-2 R2, no such significant trend towards higher reactivity with larger alkyl chains as for mouse R2 is observed. The group of *p*-alkoxyphenols react generally faster with the HSV-2 R2 tyrosyl radical than with the *E. coli* R2 radical, but much slower than with the mouse R2 radical. Reduction of the tyrosyl radical in HSV-2 R2 is slower with branched hydrophobic side groups than with the corresponding linear one, as for *E. coli* R2 (Table 1).

3.2. Reaction of the iron center in protein R2 with *p*-propoxyphenol

Optical absorption studies in the range 300–450 nm show

Table 1
Rate constants for the reduction of the tyrosyl radical of *E. coli*, mouse, and HSV-2 proteins R2 by *p*-alkoxyphenols and HU at 20°C

Inhibitor	k_2 ($M^{-1} \cdot s^{-1}$)[a]			
	E. coli[#] R2	Mouse R2	HSV-2 R2	Model radical[#,b]
p-Methoxyphenol	0.9 ± 0.01	28 ± 2	6 ± 1	30 ± 1
p-Ethoxyphenol	0.8 ± 0.05	54 ± 2	12.4 ± 2	25 ± 2
p-Allyloxyphenol	1.3 ± 0.05	75 ± 2	7.5 ± 1	13 ± 0.4
p-n-Propoxyphenol	1.2 ± 0.2	111 ± 3	9 ± 1	21 ± 2
p-iso-Propoxyphenol	0.4 ± 0.02 (0.54 ± 0.01)*	160 ± 4	6 ± 1	110 ± 1
o-iso-Propoxyphenol	–	9 ± 0.5	–	2 ± 0.2
p-n-Butoxyphenol	3.5 ± 0.1	267 ± 24	22 ± 2	19 ± 1
p-iso-Butoxyphenol	0.38 ± 0.01 (0.4)*	222 ± 7	9.3 ± 0.3	13 ± 0.4
Hydroxyurea	0.36 ± 0.02	1.1 ± 0.1	0.6 ± 0.05	16 ± 0.3

[a] The second order rate constants k_2 ($M^{-1} \cdot s^{-1}$) were determined by using a stopped-flow UV-vis or a EPR stopped-flow apparatus[#]. All rate constants are averages of at least five independent measurements and different charges (except HSV-2) of proteins.
[b] The model radical is potassium nitrosodisulfonate (Fremy's salt) in 50 mM HEPES, pH 7.0.

that both, the tyrosyl radical and the iron center in mouse R2 are destroyed by *p*-propoxyphenol (Fig. 1B). The same spectral behaviour was observed for HSV-2 R2, but not for *E. coli* R2 (data not shown). In order to study the reduction of the iron center in the three R2 proteins by the *p*-alkoxyphenols, additional experiments were performed to detect released ferrous iron. Bathophenanthroline-disulfonic acid, a ferrous iron chelator with a typical absorption band at 535 nm for the Fe^{2+}-bathophenanthroline complex [18], was added to the inhibition assay and a set of UV-vis spectra were recorded after different reaction times. Fig. 2 shows the iron release in *E. coli* (A), mouse (B), and HSV-2 (C) R2 by *p*-propoxyphenol. Whereas the band of the Fe^{2+}-bathophenanthroline complex band increases with increasing reaction time for mouse and HSV-2 R2 with *p-n*-propoxyphenol (Fig. 2A,C), this effect was not observed for *E. coli* R2 up to 120 min (Fig. 2A). In the absence of *p*-propoxyphenol, bathophenanthroline-disulfonic acid has a negligible effect on the three R2 proteins (data not shown). The kinetics of formation of the Fe^{2+}–bathophenanthroline complex in mouse R2 (Fig. 2B) and HSV-2 R2 (Fig. 2C) exhibit $t_{1/2}$ of 22 min and 39 min, respectively. From the molar extinction coefficient for the Fe^{2+}–bathophenanthroline complex (ε_{535} = 22,000 $M^{-1} \cdot cm^{-1}$ [18]) a final concentration of the released iron of 88% and 31% from mouse and HSV-2 R2, respectively, was determined (100% refer to four iron molecules per R2). The low iron content in HSV-2 R2 (31%) estimated from the Fe^{2+}–bathophenanthroline complex may be explained by the 3-fold lower affinity of the virus protein for iron, produced in a procaryotic expression system with the pET-R2 vector [19].

After removing the inhibitor by gel filtration, mouse R2 could be reconstituted using the anaerobic iron/oxygen procedure (see Materials and Methods). The tyrosyl radical reappeared instantaneously. The intensity of the g = 2.0 EPR signal was approximately 90% of the original signal. This indicates that no irreversible process takes place in the protein during inactivation of protein R2 by *p*-alkoxyphenols.

3.3. Reduction of the model radical Fremy's salt

The reaction of *p*-alkoxyphenols with a stable model free radical, potassium nitrosodisulfonate (Fremy's salt), was also studied. The EPR spectrum of this radical shows three narrow hyperfine lines from the nitrogen nucleus (I = 1). The time course of reducing the model radical by the R2-inhibitors was followed from the top of the high-field line of its EPR spectrum after 1:1 mixing with the inhibitor in the EPR stopped-flow apparatus. The rate of quenching the Fremy radical by all *p*-alkoxyphenols and hydroxyurea follows pseudo-first order kinetics (inhibitor concentration in excess). The rate constants of the reduction of the model radical by *p*-alkoxyphenols at pH 7 are in the same order of magnitude between 13 and 30 $M^{-1} \cdot s^{-1}$ (except *p-iso*-propoxyphenol) and comparable with the more common R2-inhibitor HU (k_2 = 16 $M^{-1} \cdot s^{-1}$) (Table 1). The reactivities of nearly all *p*-alkoxyphenols towards the model radical are independent on alkyl chain length, except *p-iso*-propoxyphenol. So far there is no explanation for the five times higher reactivity of quenching the model radical by *p-iso*-propoxyphenol compared with the other *p*-alkoxyphenols. The rate of reaction of the *p*-alkoxyphenols with the protein-free model radical is obviously different in comparison with the reactivity with the protein-linked tyrosyl radical in R2 of RR (Table 1), particularly in case of the mouse R2 protein.

4. Discussion

Previous studies of inhibitors to protein R2 of the one-electron reduction type have suggested at least three possible mechanisms for inhibitor activity: (i) direct accessibility of the inhibitor to the iron/radical site, perhaps mediated by protein conformational flexibility, (ii) long range electron transfer from an interaction site on or close to the protein surface, or (iii) existence of another more accessible free radical in equilibrium with the tyrosyl radical [7,20,21]. At present it is not possible to unambigously distinguish a common dominating mechanism for the different R2 proteins that have been studied. The crystal structure of the *E. coli* R2 suggests that molecules larger than O_2 cannot access the radical site [22], arguing against an access mechanism. The structure of the mouse and HSV proteins could, however, be more open. There is no evidence of saturation of the inhibition rate at high *p*-methoxyphenol (data not shown) and HU concentrations [11,17], arguing against the electron transfer mechanism. There is no direct spectroscopic evidence for an additional radical in protein R2 [20]. In fact the different mechanisms mentioned above could contribute in parallel, in different proportions under different conditions.

The present results clearly show that a reasonably large hydrophobic side chain with a substituted phenyl group very significantly promotes the inhibitor activity, particularly for the mouse protein. The comparison of size restrictions is in agreement with an early study of the *E. coli* and mouse enzymes [23], which showed that the *E. coli* R2 is much more restrictive than the mouse R2 in its reactions. The reactions of various derivatives of hydrazines, hydroxylamines, and hydroxamic acids with *E. coli* R2 have shown that increasing size of the molecule in that case generally decreases the inhibitory effect, but that the presence of a hydrophobic phenyl group increases the reactivity of the inhibitor [21,24]. This agrees with the present observations. The reduction of iron in parallel with the radical has also been previously observed for mouse and HSV enzymes with HU and catechol, respectively, in agreement with our results [11,12,25].

The specific requirements for a hydrophobic *p*-substituted phenyl group for high inhibitory activity suggests a rather specific interaction with an hydrophobic site in the protein. The different reactivities of the *E. coli*, mouse, and virus proteins should arise from structural differences between the proteins, and most likely a more accessible interaction site in the mouse protein. From the available data one cannot conclude whether this site is situated in the hydrophobic environment of the tyrosyl radical or if it is another site inside or outside of the protein. Nevertheless, the *p*-substituted alkoxyphenols represent a new class of very potent inhibitors of mammalian RR, with activity against the essential tyrosyl radical in purified protein as well as in tumor cells [10,26], with possible importance for depleting deoxyribonucleotide pools in HIV-infected cells [27].

Acknowledgements: We thank Prof. B.-M. Sjöberg and Prof. L. Thelander for the generous gifts of the *E. coli* strain overproducing the *E. coli* R2 and the *E. coli* strain containing the mouse R2 gene, respectively. This work was supported by the Deutsche Forschungsgemeinschaft (Projekt 751/1–2) and the Swedish Natural Science Research Council.

References

[1] Thelander, L. and Reichard, P. (1979) Annu. Rev. Biochem. 48, 133–158.
[2] Lammers, M. and Follmann, H. (1983) Structure and Bonding 54, 27–91.
[3] Gräslund, A., Sahlin, M. and Sjöberg, B.-M. (1985) Environ. Health Perspect. 64, 139–149.
[4] Petersson, L., Gräslund, A., Ehrenberg, A., Sjöberg, B.-M. and Reichard, P. (1980) J. Biol. Chem. 255, 6706–6712.
[5] Stubbe, J. (1990) Adv. Enzymol. 63, 349–419.
[6] Ehrenberg, A. and Reichard, P. (1972) J. Biol. Chem. 11, 3485–3488.
[7] Nordlund, P., Sjöberg, B.-M. and Eklund, H. (1990) Nature 345, 593–598.
[8] Eriksson, S., Gräslund, A., Skog, S., Thelander, L. and Tribukait, B. (1984) J. Biol. Chem. 259, 11695–11700.
[9] Morgan, B.D.G., O'Neill, T., Dewey, D.L., Galpine, A.R. and Riley, P.A. (1981) Clin. Oncol. 7, 227–234.
[10] Pötsch, S., Drechsler, H., Liermann, B., Gräslund, A. and Lassmann, G. (1994) Mol. Pharmacol. 45, 792–796.
[11] Nyholm, S., Thelander, L. and Gräslund, A. (1993) Biochemistry 32, 11569–11574.
[12] Atta, M., Lamarche, N., Battioni, J.P., Massie, B., Langelier, Y., Mansuy, D. and Fontecave, M. (1993) Biochem. J. 290, 807–810.
[13] Sjöberg, B.-M., Hahne, S., Karlsson, M., Jörnvall, H., Göransson, M. and Uhlin, B.E. (1986) J. Biol. Chem. 261, 5658–5662.
[14] Mann, G.J., Gräslund, A., Ochiai, E., Ingemarson, R. and Thelander, L. (1991) Biochemistry 30, 1939–1947.
[15] Ochiai, E., Mann, G.J., Gräslund, A. and Thelander, L. (1990) J. Biol. Chem. 26, 15758–15761.
[16] Bradford, M.M. (1976) Anal. Biochem. 72, 248–254.
[17] Lassmann, G., Thelander, L. and Gräslund, A. (1992) Biochem. Biophys. Res. Commun. 188, 879–887.
[18] Blair, D. and Diehl, H. (1961) Talanta 7, 163–174.
[19] Lamarche, N., Massie, B., Fontecave, M., Atta, M., Guilbault, C., Dumas, F., Gaudreau, P., Langelier, Y., to be submitted.
[20] Karlsson, M., Sahlin, M. and Sjöberg, B.-M. (1992) J. Biol. Chem. 267, 12622–12626.
[21] Gerez, C. and Fontecave, M. (1992) Biochemistry 31, 780–786.
[22] Nordlund, P. and Eklund, H. (1993) J. Mol. Biol. 232, 123–164.
[23] Kjøller-Larsen, I., Sjöberg, B.-M. and Thelander, L. (1982) Eur. J. Biochem. 125, 75–81.
[24] Swarts, J.C., Aquino, M.A.S., Han, J.Y., Lam, K.Y. and Sykes, A.G. (1995) Biochim. Biophys. Acta 1247, 215–224.
[25] Nyholm, S., Ingemarson, R., Schmidt, P.P., Thelander, L. and Gräslund, A., to be submitted.
[26] Lassmann, G., Liermann, B., Arnold, W. and Schwabe, K. (1991) J. Cancer Res. Clin. Oncol. 117, 91–95.
[27] Lassmann, G. and Pötsch, S. (1993) German patent P 43 44 645.0.